

THE ABUNDANCE EVOLUTION OF OXYGEN, SODIUM, AND MAGNESIUM IN EXTREMELY METAL POOR INTERMEDIATE-MASS STARS: IMPLICATIONS FOR THE SELF-POLLUTION SCENARIO IN GLOBULAR CLUSTERS

PAVEL A. DENISSENKOV AND FALK HERWIG

Department of Physics and Astronomy, University of Victoria, P.O. Box 3055, Victoria, BC V8W 3P6, Canada;
dpa@uvastro.phys.uvic.ca, fherwig@uvastro.phys.uvic.ca

Received 2003 April 3; accepted 2003 May 8; published 2003 May 15

ABSTRACT

We present full stellar evolution and parametric models of the surface abundance evolution of ^{16}O , ^{22}Ne , ^{23}Na , and the magnesium isotopes in an extremely metal poor intermediate-mass star ($\mathcal{M}_{\text{ZAMS}} = 5 \mathcal{M}_{\odot}$, where ZAMS stands for the zero-age main sequence, and $Z = 0.0001$). ^{16}O and ^{22}Ne are injected into the envelope by the third dredge-up following thermal pulses on the asymptotic giant branch. These species and the initially present ^{24}Mg are depleted by hot bottom burning (HBB) during the interpulse phase. As a result, ^{23}Na , ^{25}Mg , and ^{26}Mg are enhanced. If the HBB temperatures are sufficiently high for this process to deplete oxygen efficiently, ^{23}Na is first produced and then depleted during the interpulse phase. Although the simultaneous depletion of ^{16}O and enhancement of ^{23}Na is possible, the required fine-tuning of the dredge-up and HBB casts some doubt on the robustness of this process as the origin of the O-Na anticorrelation observed in globular cluster stars. However, a very robust prediction of our models are low $^{24}\text{Mg}/^{25}\text{Mg}$ and $^{24}\text{Mg}/^{26}\text{Mg}$ ratios whenever significant ^{16}O depletion can be achieved. This seems to be in stark contrast to recent observations of the magnesium isotopic ratios in the globular cluster NGC 6752.

Subject headings: globular clusters: general — stars: abundances — stars: AGB and post-AGB

1. INTRODUCTION

In globular clusters (GCs) spectroscopic observations have revealed large (~ 1 dex) star-to-star abundance variations of C, N, O, Na, Mg, and Al (e.g., Ramírez & Cohen 2002). The anticorrelations of C-N, O-Na, and Mg-Al point to the simultaneous operation of the CNO, NeNa, and MgAl cycles. In the so-called *evolutionary scenario*, it is assumed that these abundance variations are produced in the vicinity of the hydrogen-burning shell in red giant branch (RGB) stars and that some extramixing transports them to the convective envelope (Denissenkov & Denisenkova 1990; Langer, Hoffman, & Sneden 1993; Denissenkov & Weiss 2001).

The evolutionary scenario has been challenged by the recent discovery of C-N, O-Na, and even Mg-Al anticorrelations in the main sequence (MS), MS turnoff, and subgiant stars in the GCs 47 Tucanae and NGC 6752 (Harbeck, Smith, & Grebel 2003; Gratton et al. 2001; Grundahl et al. 2002). A likely origin of these abundance anomalies is pollution by material processed via H burning in more evolved stars. In this *primordial scenario*, intermediate-mass stars (IMs; $\mathcal{M} \approx 3\text{--}8 \mathcal{M}_{\odot}$) in their asymptotic giant branch (AGB) evolution phase have been proposed as contaminators (Ventura et al. 2001; Ventura, D’Antona, & Mazzitelli 2002).

Thermally pulsing (TP)–AGB stars process material in an He-burning shell and in an H-burning shell. The H shell dominates the energy production most of the time. However, recurrent thermonuclear He-shell flashes drive a temporary (~ 10 yr) pulse-driven convective zone (PDCZ) that encompasses the entire region between the He-burning shell and the H-burning shell (the intershell). Immediately after the end of the thermal pulsing, the base of the convective envelope begins to move inward in mass, and eventually material from below the H shell is dredged up to the envelope (the third dredge-up [TDU]). During the interpulse period in massive AGB stars, hot bottom burning (HBB) further modifies the envelope chemical composition (Boothroyd, Sackmann, & Ahern 1993).

In the evolutionary scenario, Al can be synthesized on the RGB if some low-mass stars in GCs were initially enriched with ^{25}Mg , possibly from massive AGB stars (Denissenkov et al. 1998; Denissenkov & Weiss 2001). In this *combined scenario*, star-to-star abundance variations of C, N, O, Na, Mg, and Al in GCs may have multiple origins: (1) on the MS, they may be due to pollution in the past either by the massive AGB stars or by somewhat more massive ($0.9 \leq \mathcal{M}/\mathcal{M}_{\odot} \leq 2$) RGB stars than the present-day MS turnoff stars that had undergone deep extramixing, and (2) on the RGB, they may be partly tracers of the same pollution that occurred on the MS and partly (in the most rapidly rotating stars) they may be due to deep extramixing (Denissenkov & Weiss 2001; Denissenkov & Vandenberg 2003).

In the primordial scenario, massive AGB stars are thought to be responsible for very low O abundances ($[\text{O}/\text{Fe}] \leq -0.5$, down from the assumed initial value of $+0.4$) in MS stars in GCs as a result of *pollution with O-depleted material*. Indeed, Ventura et al. (2001, 2002) have reported that in metal-poor massive AGB stars, HBB may be capable of producing the required O depletion. However, nucleosynthesis beyond the CNO cycle has not been investigated yet. In this Letter, we will take into account all of the cycles of nuclear reactions participating in the H burning as well as the effect of the TDU. In § 2, we present the abundances from full stellar evolution models. In § 3, an equivalent parametric AGB model is described. In § 4, we discuss the results of calculations with the parametric models and make our final conclusions.

2. FULL STELLAR EVOLUTION MODELS

Our one-dimensional stellar evolution code (Herwig 2000) includes updated opacities (Iglesias & Rogers 1996; Alexander & Ferguson 1994) and a nuclear network with all relevant reactions, with the rates for the NeNa cycle reactions taken from El Eid & Champagne (1995). A simultaneous, fully implicit, iterative solution of the nuclear network and time-dependent mixing equations for each isotope (Herwig 2001)

and hydrodynamic overshooting with a geometric, exponential decay parameter f can be included. We have improved the adaptive time-step and grid-allocation algorithm for the extremely metal poor models in order to ensure that the TDU properties are not affected by numerical resolution issues. The mixing-length parameter is $\alpha_{\text{MLT}} = 1.7$ from calibrating a solar model, and $X(^4\text{He})_{\text{init}} = 0.23$.

We choose a model of initially $5 M_{\odot}$ with a metallicity of $Z = 0.0001$ as a representative example for IMS that might have polluted GC stars of the lowest metallicity ($[\text{Fe}/\text{H}] \approx \log(Z/Z_{\odot}) = -2.3$). We evolve the initial pre-MS model through all evolutionary phases, and details will be presented in a forthcoming paper. Up to the first thermal pulse on the AGB, exponential overshooting with $f = 0.016$ has been considered at all convective boundaries. The first envelope abundance alteration occurs as a result of the second dredge-up. Material processed mainly by H-shell burning is brought to the surface. ^{23}Na is enhanced by 0.75 dex from the conversion of the initial abundance of ^{22}Ne and some ^{20}Ne . ^{16}O is depleted by 0.1 dex because of the action of the ON cycle. Magnesium isotopes are changed by less than 0.05, 0.1, and 0.01 dex for mass numbers 24, 25 and 26 in the second dredge-up.

During the TP-AGB phase, the interplay of the TDU and HBB alters the envelope abundances. The TDU brings ^{22}Ne and a rather uncertain amount of ^{16}O to the surface. ^{25}Mg and ^{26}Mg are produced by two processes: (1) by HBB in the envelope (at the expense of ^{24}Mg) and (2) by α -captures on ^{22}Ne in the PDCZ. The second process is important when the temperature in the PDCZ exceeds $\sim 3.5 \times 10^8$ K. The HBB also destroys ^{16}O (and produces ^{17}O), while ^{23}Na is produced by proton captures on the dredged-up ^{22}Ne . At higher temperatures, ^{23}Na can be destroyed again. The overall budget of the O, Na, and Mg isotopes depends on the interplay of dredge-up and HBB. In addition, mass loss plays an important role. It limits the TP-AGB evolution time with a high HBB temperature and an efficient third dredge-up.

All of these effects can be observed in the surface abundance evolution of two TP-AGB model sequences that we evolved from the same early-AGB model (Fig. 1). In the first sequence (Fig. 1a), we have isolated the effect of HBB by assuming no overshooting and a rather low time resolution (typically less than 1000 models per TP cycle). As a result, this sequence shows no TDU (apart from one outlier seen in the run of ^{16}O at $t = 60,000$ yr). We have also assumed mass loss according to Blöcker (1995) with $\eta_{\text{B}} = 0.1$, and the model experiences 43 thermal pulses until the envelope mass is lost. This sequence shows a large ^{16}O depletion, but due to the lack of ^{22}Ne dredge-up, ^{23}Na is depleted as well.

In Figure 1b, a model is shown in which we have considered only negligible overshooting at the bottom of the He-flash convection zone ($f = 0.002$; the intershell abundances are not affected significantly by this very small PDCZ overshoot). At the bottom of the envelope convection, we have assumed $f = 0.016$, as calibrated at the MS core convection boundary. Here we have used the high spatial and time resolution required to model the TDU. Mass loss has been turned off for this case in order to explore the largest possible nuclear enrichment by HBB and dredge-up. After a few thermal pulses, the TDU is very efficient, and it reaches into ^{16}O -rich layers below the zones previously covered by the PDCZ. Our models with this deep dredge-up show systematically higher HBB temperatures than the model without dredge-up. The unusually deep dredge-up is likely related to the effect of sustained, fierce H burning in the overshoot layer. We will discuss the details of this effect,

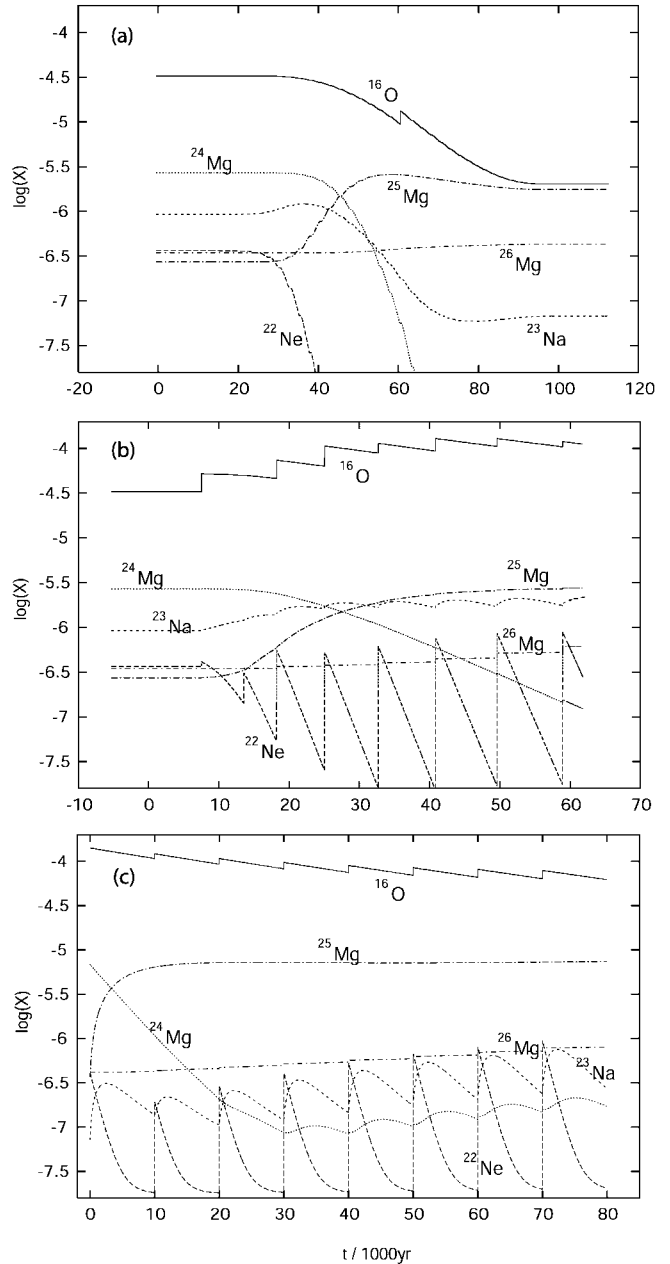


FIG. 1.—Envelope abundance evolution for two full TP-AGB stellar model sequences with $M_{\text{ZAMS}} = 5 M_{\odot}$, where ZAMS stands for the zero-age main sequence, and $Z = 0.0001$ (panels a and b, respectively). The sequences are distinguished by differing assumptions concerning the mixing and the numerical time resolution, as discussed in the text. Panel c shows the envelope abundance evolution for our parametric AGB model with $T_{\text{HBB}} = 10^8$ K and $\lambda = 1$. In all panels, $t = 0$ corresponds to the first thermal pulse.

which is unique to very metal poor IMSs, in a forthcoming paper. For the present study, it is sufficient to note that the TDU in these stars could be much more efficient than previous models without overshooting indicated (e.g., Ventura et al. 2002) and that oxygen could be enhanced by this process. This undermines the ability of HBB to deplete oxygen in the envelope. However, with efficient TDU, ^{22}Ne is dredged up, and ^{23}Na is, in fact, further increased. The behavior of the magnesium isotopes is qualitatively the same as in the model without dredge-up, indicating that these species are mainly affected by the HBB.

According to our high-resolution, full stellar evolution models with efficient TDU, massive AGB stars *cannot* show si-

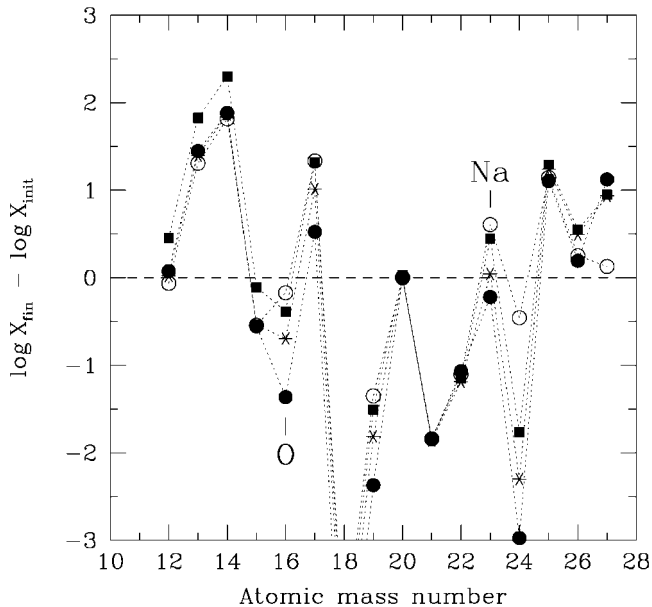


FIG. 2.—Final envelope abundances with respect to the initial ones after eight thermal pulses calculated with the parametric AGB model: (λ , T_{HBB}) = (1, 10^8 K) (filled squares), (0.3, 9×10^7 K) (open circles), (0.3, 10^8 K) (asterisks), and (0.3, 1.1×10^8 K) (filled circles).

multaneously ^{16}O depletion and Na enhancement. Using parametric models, we will now explore intermediate cases with ^{22}Ne dredge-up but limited ^{16}O dredge-up, and we will consider in more detail the evolution of magnesium isotopes.

3. PARAMETRIC MODELS

We have developed a parametric nucleosynthesis and mixing code for massive AGB stars. All processes that are relevant for the abundance evolution of O, Na, and the Mg isotopes are considered. In particular, we include the effects of HBB and dredge-up, as well as mixing and burning in the PDCZ. Most reaction rates are taken from the NACRE (Nuclear Astrophysics Compilation of REaction rates; Angulo et al. 1999) database (see Denissenkov & Tout 2003 for details). For the initial conditions, we assume scaled solar abundances, except for an enhancement of the α -elements (^{16}O , ^{20}Ne , ^{24}Mg , etc.) by +0.4 dex, and a depletion of Na and Al by the same factor, in accordance with the chemical composition of the halo dwarfs. As in the full stellar models, the metallicity is $Z = 0.0001$. In the following description, we use the subscripts “PDCZ,” “HBS,” and “HBB” to indicate the temperatures and densities at the base of the PDCZ, in the H-burning shell, and at the bottom of the convective envelope, respectively.

A TP sequence starts with a calculation of the mixing and nucleosynthesis in the PDCZ. The pre-TP composition of the intershell zone is a mixture consisting of a fraction γ of material from the preceding PDCZ and a fraction $(1 - \gamma)$ containing H-shell ashes. For the first thermal pulse, we take $\gamma = 0$. The mass ΔM_{PDCZ} of the PDCZ is divided into 25 zones with the temperature and density decreasing linearly from T_{PDCZ} and ρ_{PDCZ} at its bottom to T_{HBS} and ρ_{HBS} at its top. For the mixing in the PDCZ, which is treated as a diffusion process, we assume a constant coefficient $D_{\text{mix}} = 10^{15} \text{ cm}^2 \text{ s}^{-1}$. For the temperature T_{PDCZ} , we choose the maximum value observed in the full stellar models. For that reason, we are really modeling only the high-temperature phase of the PDCZ. The He burning is stopped every time when the mass fraction abundance of ^{12}C in the

PDCZ has reached the value 0.23, as proposed by Renzini & Voli (1981). After that, a fraction λ of the total mass ΔM_{PDCZ} of material with the final abundances from the PDCZ is added to the envelope to simulate the effect of the TDU. Then, we follow the changes of the envelope composition due to the HBB during the interpulse period Δt_{ip} . For this, we process the envelope abundance distribution after the TDU in one zone at constant T_{HBB} and $\rho_{\text{HBB}}\delta$ (a dimensionless factor δ accounts for the fact that after averaging over the mass of the convective envelope, coefficients in the nuclear kinetics network can be written in a form $\langle\sigma v\rangle(T_{\text{HBB}})N_{\text{A}}\rho_{\text{HBB}}\delta$, where $\langle\sigma v\rangle(T)N_{\text{A}}$ is a reaction rate at a temperature T and $\delta = (1 - a)^{-1} \int_a^1 (\rho/\rho_{\text{HBB}})[\langle\sigma v\rangle(T)/\langle\sigma v\rangle(T_{\text{HBB}})]dx$, with $x = M_r/M$ and $a = M_{\text{HBB}}/M$; the full stellar evolution models give $\delta \approx 10^{-5}$, which means that HBB takes place in a narrow zone adjacent to the base of the convective envelope). In addition to the HBB computation, we calculate the abundance distribution of the H-burning ashes from the new post-HBB envelope composition with another one-zone model at H-shell temperature and density. This whole sequence is repeated for eight TP cycles.

We use the following structure parameters from the full models: the CO-core mass $M_c = 0.96 M_{\odot}$, $\Delta M_{\text{PDCZ}} = 0.0025 M_{\odot}$, $T_{\text{PDCZ}} = 3.2 \times 10^8 \text{ K}$, $\rho_{\text{PDCZ}} = 5 \times 10^3 \text{ g cm}^{-3}$, $T_{\text{HBS}} = 1.2 \times 10^8 \text{ K}$, $\rho_{\text{HBS}} = 40 \text{ g cm}^{-3}$, $T_{\text{HBB}} = 10^8 \text{ K}$, $\rho_{\text{HBB}}\delta = 10^{-5} \text{ g cm}^{-3}$, and $\Delta t_{\text{ip}} = 10^4 \text{ yr}$. Our test calculations have shown that the envelope abundances depend weakly on the parameter γ for a wide range of $0.2 \leq \gamma \leq 0.6$. Therefore, its value was kept constant at $\gamma = 0.6$, as given by the full stellar evolution calculations.

The efficiency of the nuclear processing of the envelope material in the HBB is determined by three parameters: Δt_{ip} , $\rho_{\text{HBB}}\delta$, and T_{HBB} . However, while the efficiency is linearly proportional to the first two of them, it depends on a high power of T_{HBB} . Therefore, in our model, only the third parameter characterizes the efficiency of HBB. The envelope abundances are also strongly affected by the efficiency of the TDU (parameter λ). In the full stellar evolution models, λ depends critically on the efficiency of convection-induced extramixing, and T_{HBB} depends on the efficiency of convective energy transport in the envelope. In our parametric model, λ and T_{HBB} are free parameters.

4. RESULTS FROM THE PARAMETRIC MODEL AND GENERAL DISCUSSION

Parametric calculations were carried out for $\lambda = 0.3$ and 1 and for $T_{\text{HBB}} = 0.9, \dots, 1.1 \times 10^8 \text{ K}$. The time evolution of the envelope abundances (Fig. 1c) resembles the main features seen in the results of the full stellar evolution calculations: the dredge-up of ^{22}Ne , the production and destruction of Na via $^{23}\text{Na}(p, \alpha)^{20}\text{Ne}$ and $^{23}\text{Na}(p, \gamma)^{24}\text{Mg}$, the depletion of ^{24}Mg , and the production of ^{25}Mg and ^{26}Mg . ^{16}O is depleted just by HBB. In our standard parametric model, we assume that 2% of the ^{16}O mass fraction is dredged up from the CO core during every thermal pulse, in agreement with the average *minimum* predicted by the full stellar models. In the parametric model, the ^{16}O abundance becomes significantly depleted with $X_{\text{fin}}(^{16}\text{O})/X_{\text{init}}(^{16}\text{O}) \leq 0.2$ for $T_{\text{HBB}} > 10^8 \text{ K}$ and $\lambda = 0.3$ (Fig. 2). Thus, if no or very little ^{16}O is brought to the surface, then we confirm the findings of Ventura et al. (2001, 2002) that ^{16}O is efficiently destroyed by the HBB in the metal-poor massive AGB stars. However, our parametric models confirm the result of the full models that high HBB temperatures do not favor the Na production that would be required to explain the O-Na anticor-

relation in GC stars in the primordial scenario. Indeed, at $T = 10^8$ K, the sum of the rates of the reactions $^{23}\text{Na}(p, \alpha)^{20}\text{Ne}$ and $^{23}\text{Na}(p, \gamma)^{24}\text{Mg}$ is ~ 6.8 times as large as that of $^{16}\text{O}(p, \gamma)^{17}\text{F}$, the lower and upper limits of this ratio being 2.1 and 45, respectively (Angulo et al. 1999). Without the ^{22}Ne dredge-up source, which replenishes Na (as in our first full stellar evolution model), the O depletion is accompanied by Na destruction at $T = 10^8$ K.

But even with the dredge-up of ^{22}Ne , the final Na abundance in the envelope is found to be very sensitive to small variations of T_{HBB} : increasing T_{HBB} from 0.9×10^8 K to 1.1×10^8 K turns the Na production into the Na destruction (Fig. 2). Consequently, for high HBB temperatures, both O and Na may be depleted simultaneously, resulting in the O-Na correlation instead of the O-Na anticorrelation. If dredge-up of ^{16}O is as efficient as predicted by the high-resolution full stellar models with hydrodynamic overshooting, the temperatures for efficient ^{16}O depletion would definitively be too high for Na production. Furthermore, Iliadis et al. (2001) have recommended using a rate of the reaction $^{22}\text{Ne}(p, \gamma)^{23}\text{Na}$ that is by a factor of $\sim 10^{2.7}$ smaller than the value given by NACRE at $T = 10^8$ K. This makes Na production in massive AGB stars even more problematic. On the other hand, a rate of the reaction $^{22}\text{Ne}(p, \gamma)^{23}\text{Na}$ from El Eid & Champagne (1995), used in § 2, is a factor of $\sim 10^{3.9}$ larger than the NACRE value, which favors Na production. In summary, we cannot entirely rule out that contamination by massive AGB stars causes the O-Na anticorrelation in the primordial scenario. However, this seems to be very unlikely because it requires a fine-tuning of the AGB model parameters. This is not supported by the latest rate of the reaction $^{22}\text{Ne}(p, \gamma)^{23}\text{Na}$ either.

A very robust prediction of the primordial scenario can be made with respect to the magnesium isotopes. For temperatures in the vicinity of $T_{\text{HBB}} \approx 10^8$ K that allow ^{16}O depletion, the ^{24}Mg abundance is depleted in any case even more, producing ^{25}Mg and ^{26}Mg in turn. This result is consistently found in all of our models for a wide range of parameters. The evolution of ^{24}Mg in relation to ^{16}O is a robust result because (1) at $T = 10^8$ K, the ratio of the $^{24}\text{Mg}(p, \gamma)^{25}\text{Al}$ rate to the $^{16}\text{O}(p, \gamma)^{17}\text{F}$ rate is ~ 6.4 , the lower and upper limits being 3.9 and 13, respectively (Angulo et al. 1999), and (2) there is no source of ^{24}Mg in AGB stars [production of ^{24}Mg in the reaction $^{23}\text{Na}(p, \gamma)^{24}\text{Mg}$ in the HBB is unimportant].

Therefore, in the primordial scenario with massive AGB stars as the contaminants, the MS turnoff stars with $[\text{O}/\text{Fe}] \leq -0.5$ must have ^{24}Mg depleted and ^{25}Mg enhanced by more than

1 order of magnitude. Our assumed initial chemical composition has $[\text{O}/\text{Fe}] = 0.4$, $^{24}\text{Mg}/\text{Fe} = 0.4$, $^{25}\text{Mg}/\text{Fe} = 0.0$, and $^{26}\text{Mg}/\text{Fe} = 0.0$, i.e., the Mg isotopic ratios $^{24}\text{Mg} : ^{25}\text{Mg} : ^{26}\text{Mg} = 90.5 : 4.5 : 5.0$. According to those models in Figure 2 with significant O depletion, material released by massive AGB stars may have $\log(X_{\text{fin}}/X_{\text{init}}) \approx -1.0, -1.5, 1.2$, and 0.5 for O, ^{24}Mg , ^{25}Mg , and ^{26}Mg , respectively (in Fig. 2, the label ^{26}Mg represents the sum of ^{26}Mg and ^{26}Al). In low-mass RGB stars in the primordial scenario, $\sim 90\%$ of the mass of the convective envelope has to consist of this material. Accordingly, on the upper RGB, such a star would have $[\text{O}/\text{Fe}] = -0.32$, $^{24}\text{Mg}/\text{Fe} = -0.50$, $^{25}\text{Mg}/\text{Fe} = 1.2$, $^{26}\text{Mg}/\text{Fe} = 0.5$, and the Mg isotopic ratios $^{24}\text{Mg} : ^{25}\text{Mg} : ^{26}\text{Mg} = 13 : 71 : 16$.

These predictions seem to be in conflict with the results of the Mg isotopic composition analysis of RGB stars in the GC NGC 6752 reported by Yong et al. (2003). In the least polluted stars, these authors infer $^{24}\text{Mg} : ^{25}\text{Mg} : ^{26}\text{Mg} \approx 80 : 10 : 10$ and $[\text{O}/\text{Fe}] \approx 0.6$; in the most contaminated stars, they find $^{24}\text{Mg} : ^{25}\text{Mg} : ^{26}\text{Mg} \approx 60 : 10 : 30$ and $[\text{O}/\text{Fe}] \approx -0.1$. Thus, despite having O depleted by a factor of ~ 5 , the NGC 6752 red giants still exhibit the ^{24}Mg -dominated isotopic ratios. Moreover, the second most abundant isotope is ^{26}Mg instead of ^{25}Mg . We see only two possibilities to remove this disagreement within the primordial scenario: either (1) the ratio of the reaction rates of $^{24}\text{Mg}(p, \gamma)^{25}\text{Al}$ and $^{16}\text{O}(p, \gamma)^{17}\text{F}$ at $T \approx 10^8$ K is much less than the value given by Angulo et al. (1999), and at the same time the reaction $^{25}\text{Mg}(p, \gamma)^{26}\text{Al}$ is faster; or (2) the HBB temperature in massive metal-poor AGB stars is somewhat lower than 10^8 K, in which case the ^{24}Mg destruction would be suppressed (see the open circles in Fig. 2). However, in the second case, ^{16}O destruction would be suppressed as well, and ^{25}Mg (and not ^{26}Mg) could still be produced in a large amount. Therefore, we would need deep extramixing on the RGB to deplete O and to produce ^{26}Mg and probably Al (in the form of either ^{27}Al or ^{26}Al) at the expense of ^{25}Mg . This is exactly the combined scenario proposed by Denissenkov et al. (1998), with the minor modification that deep extramixing in the RGB stars slightly more massive than the present-day MS turnoff stars in GCs might have contributed to the star-to-star abundance variations as well.

We are grateful to the referee Santi Cassisi for several thoughtful comments and suggestions that have served to improve this Letter. We appreciate the support from D. A. Vandenberg through his Operating Grant from the Natural Sciences and Engineering Research Council of Canada.

REFERENCES

- Alexander, D., & Ferguson, J. 1994, *ApJ*, 437, 879
 Angulo, C., et al. 1999, *Nucl. Phys. A*, 656, 3
 Blöcker, T. 1995, *A&A*, 297, 727
 Boothroyd, A. I., Sackmann, I.-J., & Ahern, S. C. 1993, *ApJ*, 416, 762
 Denissenkov, P. A., Da Costa, G. S., Norris, J. E., & Weiss, A. 1998, *A&A*, 333, 926
 Denissenkov, P. A., & Denisenkova, S. N. 1990, *Soviet Astron. Lett.*, 16, 275
 Denissenkov, P. A., & Tout, C. A. 2003, *MNRAS*, 340, 722
 Denissenkov, P. A., & Vandenberg, D. A. 2003, *ApJ*, in press
 Denissenkov, P. A., & Weiss, A. 2001, *ApJ*, 559, L115
 El Eid, M. F., & Champagne, A. E. 1995, *ApJ*, 451, 298
 Gratton, R. G., et al. 2001, *A&A*, 369, 87
 Grundahl, F., Briley, M., Nissen, P. E., & Feltzing, S. 2002, *A&A*, 385, L14
 Harbeck, D., Smith, G. H., & Grebel, E. K. 2003, *AJ*, 125, 197
 Herwig, F. 2000, *A&A*, 360, 952
 ———. 2001, *Ap&SS*, 275, 15
 Iglesias, C. A., & Rogers, F. J. 1996, *ApJ*, 464, 943
 Iliadis, C., D'Auria, J. M., Starrfield, S., Thompson, W. J., & Wiescher, M. 2001, *ApJS*, 134, 151
 Langer, G. E., Hoffman, R., & Sneden, C. 1993, *PASP*, 105, 301
 Ramírez S. V., & Cohen, J. G. 2002, *AJ*, 123, 3277
 Renzini, A., & Voli, M. 1981, *A&A*, 94, 175
 Ventura, P., D'Antona, F., & Mazzitelli, I. 2002, *A&A*, 393, 215
 Ventura, P., D'Antona, F., Mazzitelli, I., & Gratton, R. 2001, *ApJ*, 550, L65
 Yong, D., Grundahl, F., Lambert, D. L., Nissen, P. E., & Shetrone, M. D. 2003, *A&A*, 402, 985